Reconstruction of an object from the modulus of its Fourier transform

J. R. Fienup

Environmental Research Institute of Michigan, P.O. Box 8618, Ann Arbor, Michigan 48107
Received February 23, 1978

We present a digital method for solving the phase-retrieval problem of optical-coherence theory: the reconstruction of a general object from the modulus of its Fourier transform. This technique should be useful for obtaining high-resolution imagery from interferometer data.

Ordinarily, atmospheric turbulence limits the resolution of an image obtained through a large telescope. There have been developed a number of interferometric techniques,[1] such as speckle interferometry[2] and amplitude interferometry,[3] for making diffraction-limited measurements of the modulus of the Fourier transform of a space object. Although the autocorrelation of an object can be directly computed from the Fourier modulus, the object itself generally cannot be computed without knowledge of the Fourier transform phase, except for the special cases of centro-symmetric objects and objects with nearby isolated point sources. If it were possible to reconstruct an object from the modulus of its Fourier transform, then very-high-resolution imagery could be obtained from interferometer data.

One possible method of reconstructing an object distribution from the modulus of its Fourier transform is to use the dispersion relation and the locations of the complex zeros of the Fourier modulus.[4] Another possibility is an iterative Newton–Raphson approach.[5] Neither of these two methods has proved practical for complicated two-dimensional imagery. We describe here a reconstruction method that works for general objects, even with noisy Fourier modulus data.

Let the object be $f(x)$ and its Fourier transform be

$$F(u) = |F(u)| \exp[i\psi(u)] = \mathcal{F}\{f(x)\}$$
$$\equiv \int\int_{-\infty}^{\infty} f(x) \exp(-i2\pi u \cdot x)\mathrm{d}x, \qquad (1)$$

where the vector position x represents a two-dimensional spatial coordinate and u a spatial frequency. For sky brightness objects, $f(x)$ is a real, nonnegative function. The problem is to find an object that is consistent with all the known constraints: that it be nonnegative and that the modulus of its Fourier transform equal the measured modulus, $|F(u)|$.

The problem is solved by an iterative approach, which is a modified version of the Gerchberg–Saxton algorithm that has been used in electron microscopy[6] and other applications.[7] We first modified the Gerchberg–Saxton algorithm to fit this problem merely by using a new set of object constraints, and refer to this as the error-reduction approach. We made other modifications of a fundamental nature to arrive at the more powerful input–output approach.

A block diagram of the error-reduction approach is shown in Fig. 1(a). At the kth iteration, $g_k(x)$, an estimate of the object, is Fourier transformed; the Fourier transform is made to conform to the known modulus; and the result is inverse-Fourier transformed, giving the image $g_k'(x)$. Then the iteration is completed by forming a new estimate of the object that conforms to the object-domain constraints:

$$g_{k+1}(x) = \begin{cases} g_k'(x), & x \notin \gamma \\ 0, & x \in \gamma \end{cases}, \qquad (2)$$

where the region γ includes all points at which $g'(x)$ violates the constraints. The principal constraint is that the object be nonnegative. An additional constraint that may be enforced is that the diameter may not exceed the known diameter of the object (which is half the diameter of the autocorrelation). The iterations can be started by using a sequence of random numbers for $g_1(x)$ or for $\phi_1(x)$.

The mean-squared error at each iteration can be defined in the Fourier domain by

$$E_F^2 = \frac{\int\int_{-\infty}^{\infty} [|G_k(u)| - |F(u)|]^2 \mathrm{d}u}{\int\int_{-\infty}^{\infty} |F(u)|^2 \mathrm{d}u}, \qquad (3)$$

where $G_k(u) = \mathcal{F}\{g_k(x)\}$, or in the object (image) domain by

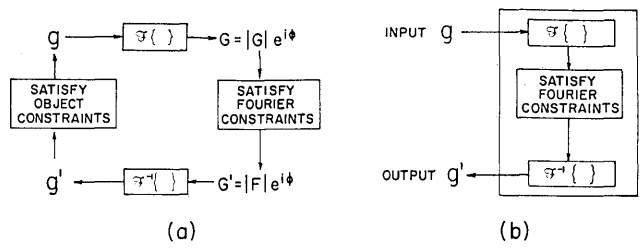

Fig. 1. (a) Block diagram of the error-reduction approach; (b) block diagram of the system for the input–output concept.

0146-9592/78/0700-0027$0.50/0

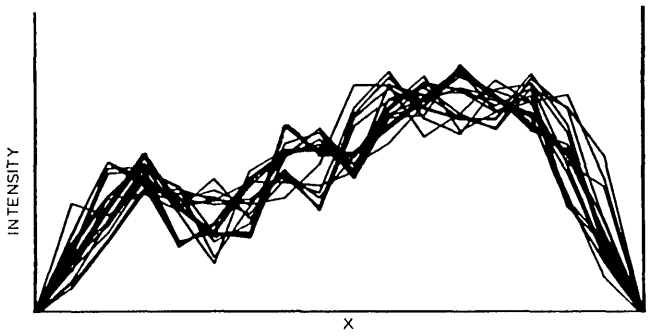

Fig. 2. Reconstruction results: test object and 15 other solutions.

$$E_0^2 = \frac{\int\int_\gamma [g_k'(x)]^2 dx}{\int\int_{-\infty}^{\infty} [g_k'(x)]^2 dx} . \quad (4)$$

In a way similar to that for the previous applications, it can be shown that the mean-squared error can only decrease at each iteration,[6,8] giving rise to the name error-reduction approach. In practice, when the error-reduction approach is used for the present application for large two-dimensional images, the mean-squared error decreases rapidly for the first few iterations but then decreases extremely slowly for later iterations, requiring an impractically large number of iterations for convergence.

In an attempt to speed up the convergence, we developed the more powerful input–output approach.[9,10] The input–output approach differs from the error-reduction approach only in the object-domain operation, and the other three operations are the same. Together, those three operations, as shown in Fig. 1(b), can be viewed as a nonlinear system having an input $g(x)$ and an output $g'(x)$. A characteristic of this system is that any output of the system has a Fourier transform with a modulus equal to $|F(u)|$. Consequently, if the output can be forced to conform to the object-domain constraints, then it is a solution to the problem. Instead of modifying the last output, as in Eq. (2), one can modify the previous input to form the new input. The principle then used is similar to that of negative feedback: compensate the input for the violation of the constraints by the output. Therefore, in order to drive the output to be nonnegative, a logical choice for the next input would be

$$g_{k+1}(x) = \begin{cases} g_k(x), & x \notin \gamma \\ g_k(x) - \beta g_k'(x), & x \in \gamma \end{cases}, \quad (5)$$

where β is a constant.

There are a number of methods of choosing $g_{k+1}(x)$, two examples of which are given in Eqs. (2) and (5), respectively, based on different points of view and different trade-offs inherent in the input–output approach. Several different methods were found to succeed. A particularly successful method of choosing $g_{k+1}(x)$ is given by the first line of Eq. (2) combined with the second line of Eq. (5). In most cases, the method of choosing $g_{k+1}(x)$ was changed after each few iterations. This periodic changing of methods after a few iterations was found to work better than using any one method for all iterations.

When the iterative approach was used on one-dimensional objects, it found multiple solutions for the same Fourier modulus data, depending on the initial input used to start the iterations. Figure 2 shows an example of an object and, superimposed, 15 different solutions (each agreeing with the Fourier modulus to within $E_F^2 < 10^{-3}$). In this case there is a uniqueness problem, but at least the various solutions correlate fairly well with the original object. For some other one-dimensional objects there is little or no similarity among the various solutions; for still others the solution is unique.

The results obtained with complicated two-dimensional objects were dramatic. Figure 3(a) shows a two-dimensional object used for experiments that resembles a sun (of diameter 52 pixels in a field of 128 × 128 pixels—only the central 80 × 80 are shown) with solar flares and sunspots. The modulus of its Fourier transform is shown in Figure 3(b). For one test of the iterative method, the initial input used was the square of random numbers shown in Figure 3(c). Figures 3(d) through 3(f) show the reconstruction results after 20, 230, and 600 iterations, respectively, having rms error $E_0 = 0.117$, 0.042, and 0.0055, respectively. In a second test, the initial input used was the circle of random numbers shown in Figure 3(g). Figures 3(h) and 3(i) show the reconstruction results of that test after 2 iterations ($E_0 = 0.111$) and 215 iterations ($E_0 = 0.019$),

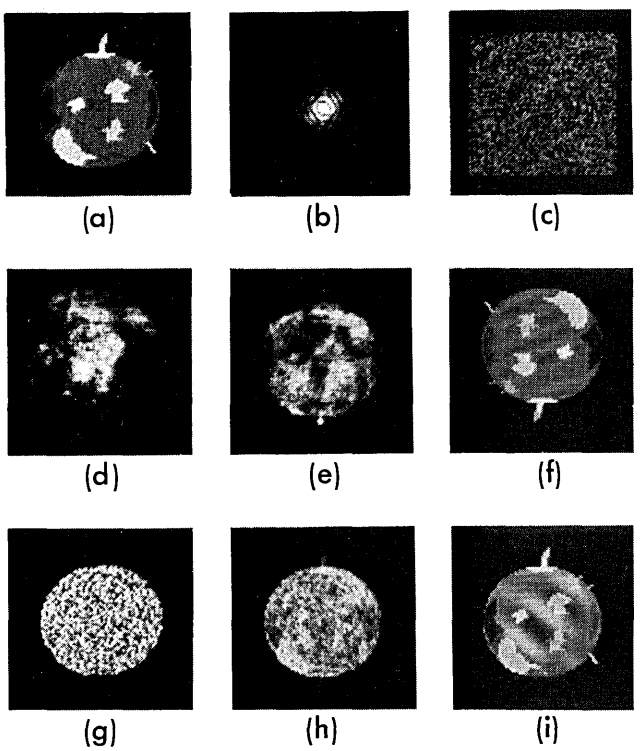

Fig. 3. (a) Test object; (b) modulus of its Fourier transform; (c) initial estimate of the object (first test); (d)–(f) reconstruction results—number of iterations: (d) 20, (e) 230, (f) 600; (g) initial estimate of the object (second test); (h)–(i) reconstruction results—number of iterations: (h) 2, (i) 215.

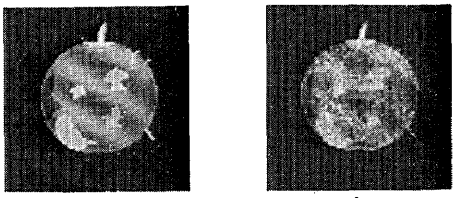

(a) (b)

Fig. 4. (a) Reconstruction result for 2.2% rms noise; (b) reconstruction result for 11% rms noise.

respectively. As a matter of economy, the iterations were halted before the error was driven to zero.

Comparing Figs. 3(f) and 3(i) with Fig. 3(a), we see that the reconstruction results differ very little from the original object. Note that inverted solutions are allowed, since $|\mathcal{F}\{f(-x)\}| = |\mathcal{F}\{f(x)\}|$. These results are significant not only because they demonstrate a method of finding solutions, but also because they suggest that the uniqueness of the result is not a serious problem for complicated two-dimensional objects.

The iterative approach has the flexibility of allowing various types of constraints or *a priori* knowledge (such as low-spatial-frequency phase information) to be enforced on the solution, which is helpful in causing the iterations to converge more rapidly and in reducing the possible ambiguities of the solution. Starting with a good initial input also helps—compare Figure 3(e) with Figures 3(h) and 3(i).

To test the sensitivity of this approach to noise, uniformly distributed random noise was added to $F(u)$, and the modulus of the resulting noisy Fourier data was used to reconstruct the object. In one test, the ratio of the rms noise to the Fourier modulus was 18% at the highest spatial frequencies [where, as seen from Fig. 3(b), the signal is weakest] and 2.2% overall. The initial input used was the same as in Fig. 3(g). Figure 4(a) shows the reconstruction result after 210 iterations ($E_0 = 0.020$). This amount of noise degraded the reconstruction only slightly. In another test, the relative rms noise was 91% at the highest spatial frequencies and 11% overall. Figure 4(b) shows the result after 300 iterations ($E_0 = 0.059$). In this case the fine details of the original object were lost; nevertheless, the gross features of the object (the low-spatial-frequency information) were still reconstructed.

We have demonstrated an iterative approach to reconstructing a general object from the modulus of its Fourier transform. This data-processing method represents a solution to the phase problem of optical coherence theory and would allow the imaging of space objects through the turbulent atmosphere using interferometer data. It is relatively fast, making it practical for use on large two-dimensional images. It is not highly sensitive to noise. Experimental results suggest that the uniqueness problem is severe for one-dimensional objects but may not be severe for complicated two-dimensional objects. The error-reduction approach, a modification of the Gerchberg–Saxton algorithm, was only partially successful; the more powerful input–output approach achieved much faster convergence. These iterative approaches should be valuable for a number of other problems in optics in which only partial information is known in each of two domains.

This work was begun under the direction of J. W. Goodman at Stanford University, where the one-dimensional results were obtained[10]; the two-dimensional results were obtained at ERIM under an internal research and development program. Portions of this paper were delivered at the October 1977 Annual Meeting of the Optical Society of America in Toronto, Canada.

References

1. R. H. T. Bates, IEEE Trans. Comput. **C-24,** 449 (1975).
2. A. Labeyrie, Astron. Astrophys. **6,** 85 (1970); D. Y. Gezari, A. Labeyrie, and R. V. Stachnik, Astrophys. Lett. **173,** L1 (1972).
3. D. G. Currie, S. L. Knapp, and K. M. Liewer, Astrophys. J. **187,** 131 (1974).
4. For a list of references, see Ref. 4 in D. Kohler and L. Mandel, J. Opt. Soc. Am. **63,** 134 (1973).
5. B. R. Frieden and D. G. Currie, J. Opt. Soc. Am. **66,** 1111A (1976).
6. R. W. Gerchberg and W. O. Saxton, Optik **35,** 237 (1972).
7. N. C. Gallagher and B. Liu, Appl. Opt. **12,** 2328 (1973); R. W. Gerchberg, Opt. Acta **21,** 709 (1974).
8. B. Liu and N. C. Gallagher, Appl. Opt. **13,** 2470 (1974).
9. J. R. Fienup, J. Opt. Soc. Am. **64,** 1395A (1974).
10. J. R. Fienup, Ph.D. thesis, Stanford University, May 1975 (University Microfilms No. 75-25523), Chap. 5.